

## 2.3 OBSERVED SITE EFFECT AND MICROTREMOR MEASUREMENT

The influence of local geologic and soil conditions on the intensity of ground shaking was recognized through this reconnaissance. Local site effects seem to have been responsible for severe damage to dwellings in this earthquake.

### *Tacna*

This city spreads along a dry valley extending from Northeast to Southwest. Tops of hills on both sides of the city are completely flat and about of the same level. Soils making up the hills are mostly pumice and weakly cemented tuff.

The northeast area, which has been being developed since 1980's along the northwestern hillside, was the most seriously damaged. Most dwellings there were RC framed with infill walls of mortar blocks and/or bricks (**Figure 2.9**).

Utility poles (5m tall) are embedded upright in concrete-paved sidewalk. Cracks developing outwardly on the pavement from these poles were mapped. Some poles are very close to the step-shaped edge of the sidewalk. The thin cover concrete thus might have affected the crack pattern. Though the number of the examined utility poles is not sufficient for thorough statistical manipulations, some poles seem to have been forcibly shaken in about Northwest –Southeast direction, transverse direction of the valley (**Figure 2.10**).



**Figure 2.9**

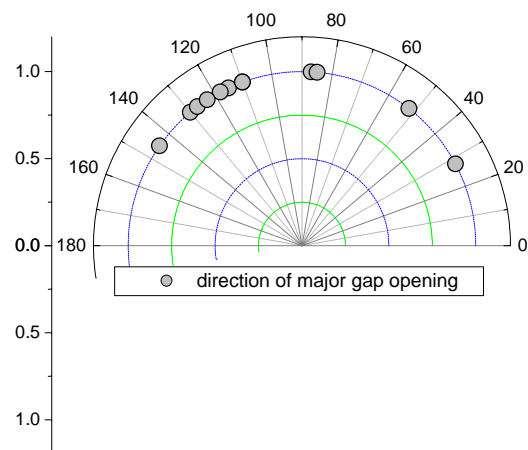


**Figure 2.10** Directions of major gap openings at bottom ends of utility poles (Tacna)

### *Moquega*

#### (1) San Francisco area

Moquega was the hardest hit city by this earthquake. A number of adobe buildings collapsed in the downtown area and many others sustained heavy damage. A thin mountain ridge, the northeast extension of a sand rock terrace rising behind the central area of Moquegua city, dips gently towards northeast. This ridge is densely covered with adobe dwellings, and the damage to dwellings was the severest there (**Figure 2.11**).

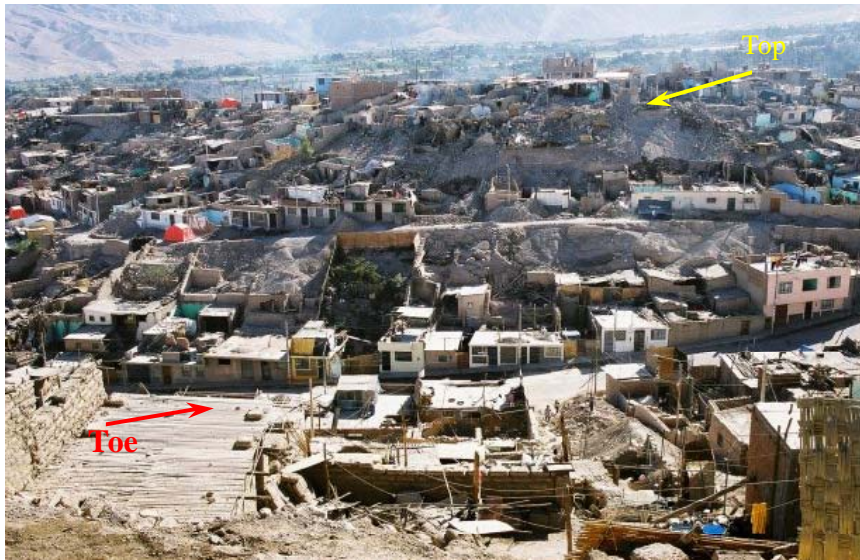


**Figure 2.11** View of the terrace next to San Francisco hill

Distribution of cracked utility poles is considered to be a good index for discussing possible spatial distribution of intense ground motions. Observed crack intensities on total 59 utility poles were roughly classified into the following 4 groups:

- Group 1:** no visible crack.
- Group 2:** with hair cracks ( $>0.1$  mm)
- Group 3:** with cracks (0.1-0.3 mm)
- Group 4:** with cracks ( $<0.3$  mm) that can be seen at a distance of about 2m

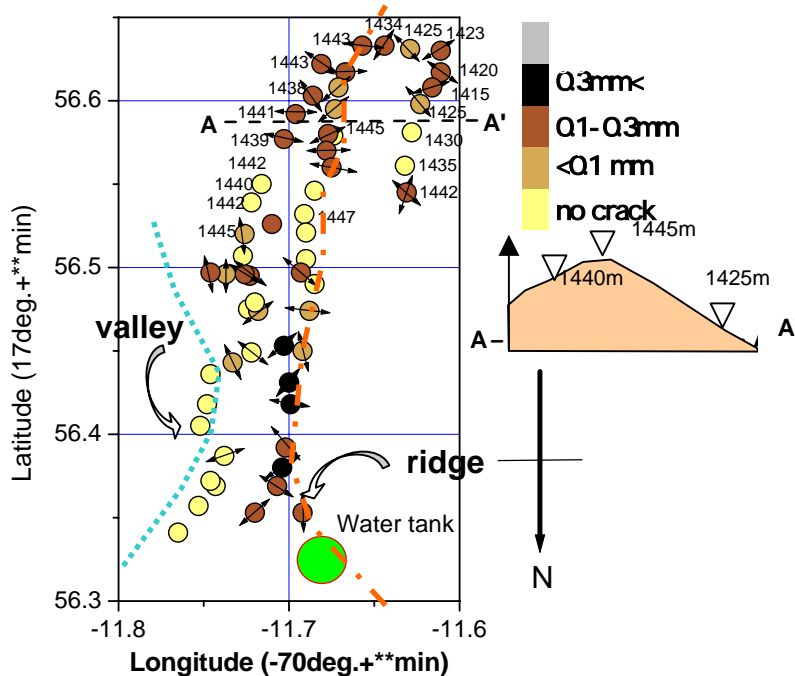


**Figure 2.12.** Distribution of cracked utility poles in San Francisco area, Moquega: Numbers put by circles show elevations of utility poles measured by using a GPS receiver.

**Figure 2.12** shows the observed distribution of crack intensities. Arrows indicate the inferred directions of strong ground motions. In this figure, the first, second and third lines from left to right lined up with the inspected utility poles are streets along a narrow valley, along the ridge and on the other hillside, respectively. It is noted that no utility pole along the valley was cracked while those around the highest peak of the ridge near a water tank (green solid circle) were severely cracked. This contrast suggests that some topographical effect must have been responsible for amplifying ground motions. The arrows along the ridge show that the effect was more pronounced in the transverse direction of the ridge.

In order to evaluate local site conditions, microtremors were measured at various locations in Moquegua and Arequipa. This technique allows identifying ground motion amplification due to topographical effects, characterizing the stiffness of the soil deposit, and identifying the site predominant period.

**Figure 2.13** presents the locations where free field microtremors were measured at Moquegua. In order to assess the site predominant frequency, the H/V ratio was used [Nakamura, 2000]. The square root of the sum of the squares of the H/V ratio for NS and EW component is shown at each position. Blue thin curves correspond to a 40.96sec-measurement whereas the thick red curve represents the average of all the measurements. A particularly low frequency site is “S” where the predominant frequency is approximately 0.6Hz. On the other hand, site “14” has a high predominant frequency equal to 8Hz.

The square root of the sum of the squares is a good index when fairly flat and horizontally layered sites are considered. However, at hilly sites, it is more meaningful to study the vibration in the directions perpendicular and parallel to the ridge independently. One of the areas most affected by the 2001 Atico Earthquake was San Francisco. Measurements were done at the toe and top of the hill (See **Figure 2.11**). The results of the spectral analysis are presented in **Figure 2.14**.

From **Figure 2.14**, it is clear that larger vibrations were recorded on top of the hill, particularly in the direction perpendicular to the ridge. In order to approximately assess the fundamental period of the hill, the microtremor spectra on the top of the hill was divided by the spectra at the toe. The results are shown in **Figure 2.15**.

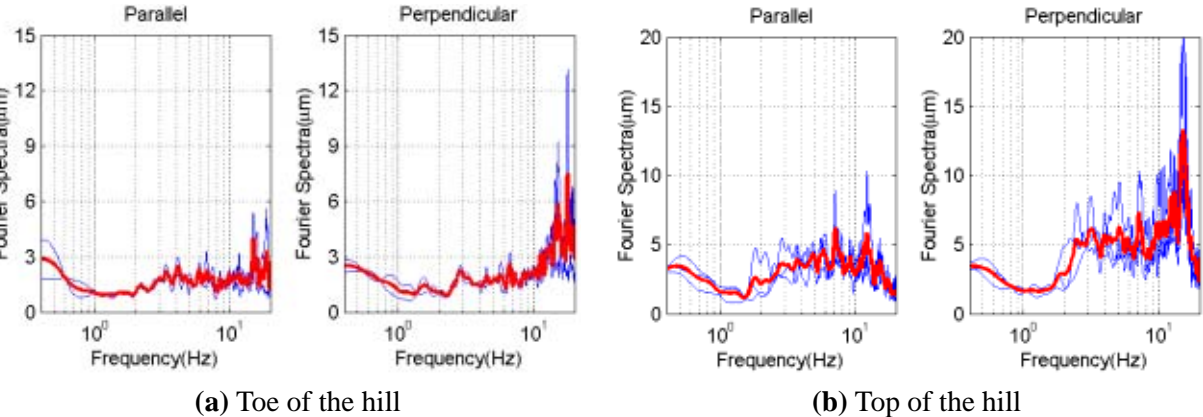


**Figure 2.14** Fourier Spectra of the microtremor measurements at San Francisco, Moquegua

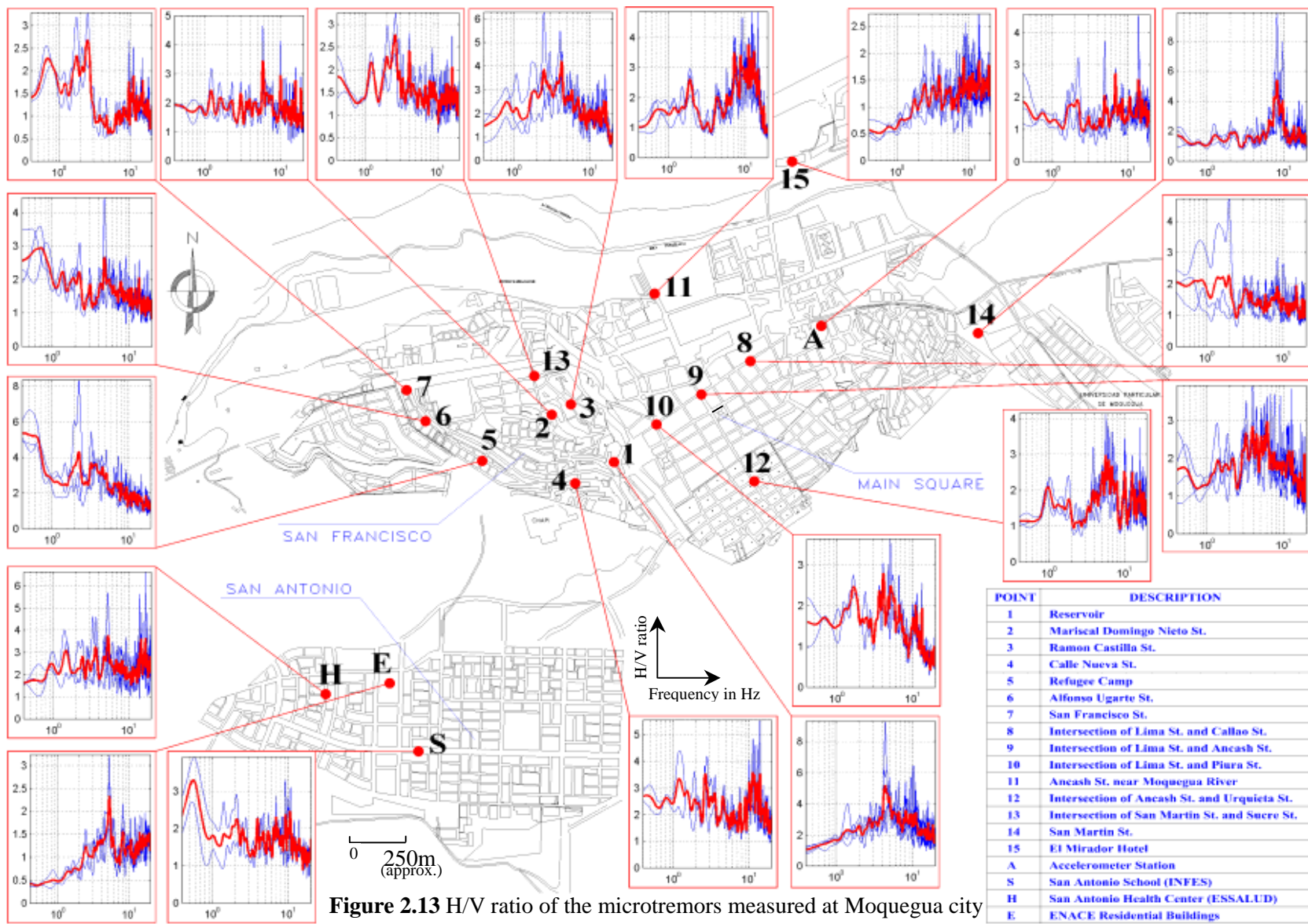
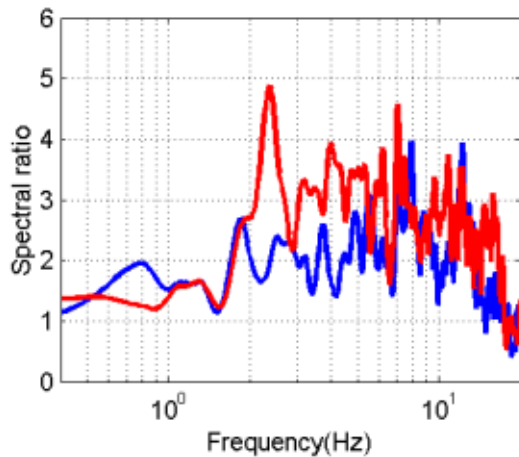


Figure 2.13 H/V ratio of the microtremors measured at Moquegua city



**Figure 2.14** Ratio of the spectra on top and at the toe of the hill. (blue: parallel to the ridge, red: perpendicular to the ridge)

**Figure 2.14** shows that larger amplification is observed in the direction perpendicular to the ridge. Furthermore, the predominant frequency in this direction, approximately 2.5Hz, is lower than the predominant frequency in the direction parallel to the ridge, 7Hz. This is consistent with the hill being more flexible perpendicularly to the ridge.

Measurements were also carried out at Moquegua and Arequipa accelerometer stations. **Figure 2.15** presents the results of the spectral analysis, which clearly show predominant frequencies of 7 and 1.1 Hz at Moquegua and Arequipa, respectively. Although there is a peak around 20Hz at the Arequipa station, this component might have been caused by some external source. When comparing this spectrum with other free field measurements in the vicinity of the station, such peak is not observed. In general, amplification at Arequipa station is larger than at Moquegua station. Note that the latter corresponds to the site where the only record of the main shock of the Atico Earthquake was recorded.

During the JSCE Team Reconnaissance survey, a large number of microtremors was registered mainly at Moquegua and Arequipa. **Table 2.1** shows a detailed list of the measurements, which are available upon request to the JSCE (<http://www.jsce.go.jp>).

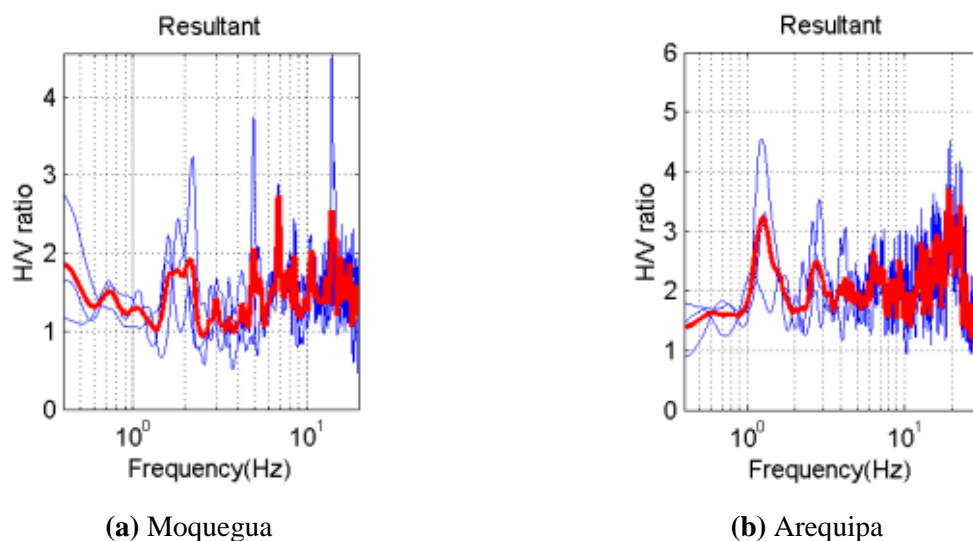


**Figure 2.15** Resultant H/V ratio at accelerometer stations

**Table 2.1** List of Microtremor measurements

Measurement ID	Location	Coordinates		Number of records	Remarks
1	Moquegua	S17°11.701'	W70°56.378'	4	Reservoir at San Francisco on top of a hill
2	Moquegua	S17°11.657'	W70°56.502'	3	Domingo Nieto St. at San Francisco at the toe of a hill
3	Moquegua	S17°11.626'	W70°56.447'	3	Ramon Castilla St. at San Francisco on top of a hill
4	Moquegua	S17°11.797'	W70°56.460'	4	Calle Nueva St.
5	Moquegua	S17°11.779'	W70°56.682'	5	Refugee camp at San Francisco
6	Moquegua	S17°11.675'	W70°56.864'	3	Alfonso Ugarte St.
7	Moquegua	S17°11.505'	W70°50.742'	5	San Francisco St.
8	Moquegua	S17°11.491'	W70°55.992'	4	Intersection of Lima St. and Callao St.
9	Moquegua	S17°11.589'	W70°56.144'	4	Intersection of Lima St. and Ancash St.
10	Moquegua	S17°11.649'	W70°55.243'	4	Intersection of Lima St. and Piura St.
11	Moquegua	S17°11.325'	W70°56.232'	4	Ancash St. near Moquegua River
12	Moquegua	S17°11.806'	W70°55.967'	5	Intersection of Ancash St. and Urquieta St.
13	Moquegua	S17°11.508'	W70°56.588'	5	Intersection of San Martin St. and Sucre St.
14	Moquegua	S17°11.362'	W70°55.519'	4	San Martin St.
15	Moquegua	S17°10.946'	W70°55.854'	4	El Mirador Hotel
San Antonio School	Moquegua	S17°12.509'	W70°56.658'	14	Free field; Laboratory and teachers' room, 2 stories; High school classrooms, 2 stories; and Building in front of High school classrooms, 1 story
Residential Buildings	Moquegua	S17°12.526'	W70°56.845'	6	Free field and 4-story residential buildings
San Antonio Accelerometer	Moquegua	S17°12.604'	W70°56.804'	5	Free field next to San Antonio Health Center
	Moquegua	S17°11.205'	W70°55.717'	4	Accelerometer at Moquegua
Chechen	Moquegua	Various	Various	39	10 locations at Chechen new development area
La Punta	Camana	S16°39.308'	W72°40.655'	13	Free field and dynamic characteristics of a utility pole at tsunami affected area
La Salle School	Arequipa	S16°24.036'	W71°31.514'	9	Free field and entrance building
Accelerometer	Arequipa	S16°24.257'	W71°31.461'	4	Arequipa accelerometer station
UMSA	Arequipa	S16°24.304'	W71°31.503'	8	Free field and Civil Engineering Building
Villa Buildings	Arequipa	S16°25.363'	W71°31.171'	11	Free field and 14-story residential buildings
Lara	Arequipa	Not available	Not available	10	Free field and dynamic characteristics of a utility pole
Hospital "Honorio Delgado"	Arequipa	S16°24.969'	W71°31.914'	19	Free field; Building III, 6 stories; Building II, 6 stories; Building IV, 6 stories; and Building VII, 4 stories
Cathedral	Arequipa	S16°23.883'	W71°32.203'	6	Over the dome and over a column



**MOQUEGUA (Figure 2.16: Bellido and Landa, 1998)**

In the northern part of Mogeegua, folded Cretaceous sedimentary rocks (Torquepara and Inagoya Formation) and Cretaceous intrusive rocks are widely cropping out. The Plio-Miocene Moquegua Formation, consist of sedimentary rocks, distributes in the southern part of Moquegua. The Quaternary alluvial and fluvial deposits, unconformably overlying the Moquegua Formation, are distributed in the city of Moquegua. The geologic succession of the city of Moquegua consist of Cretaceous hard rocks with thin younger sediments cover. From geologic point of view, the city of Moquegua has good ground condition against shaking.

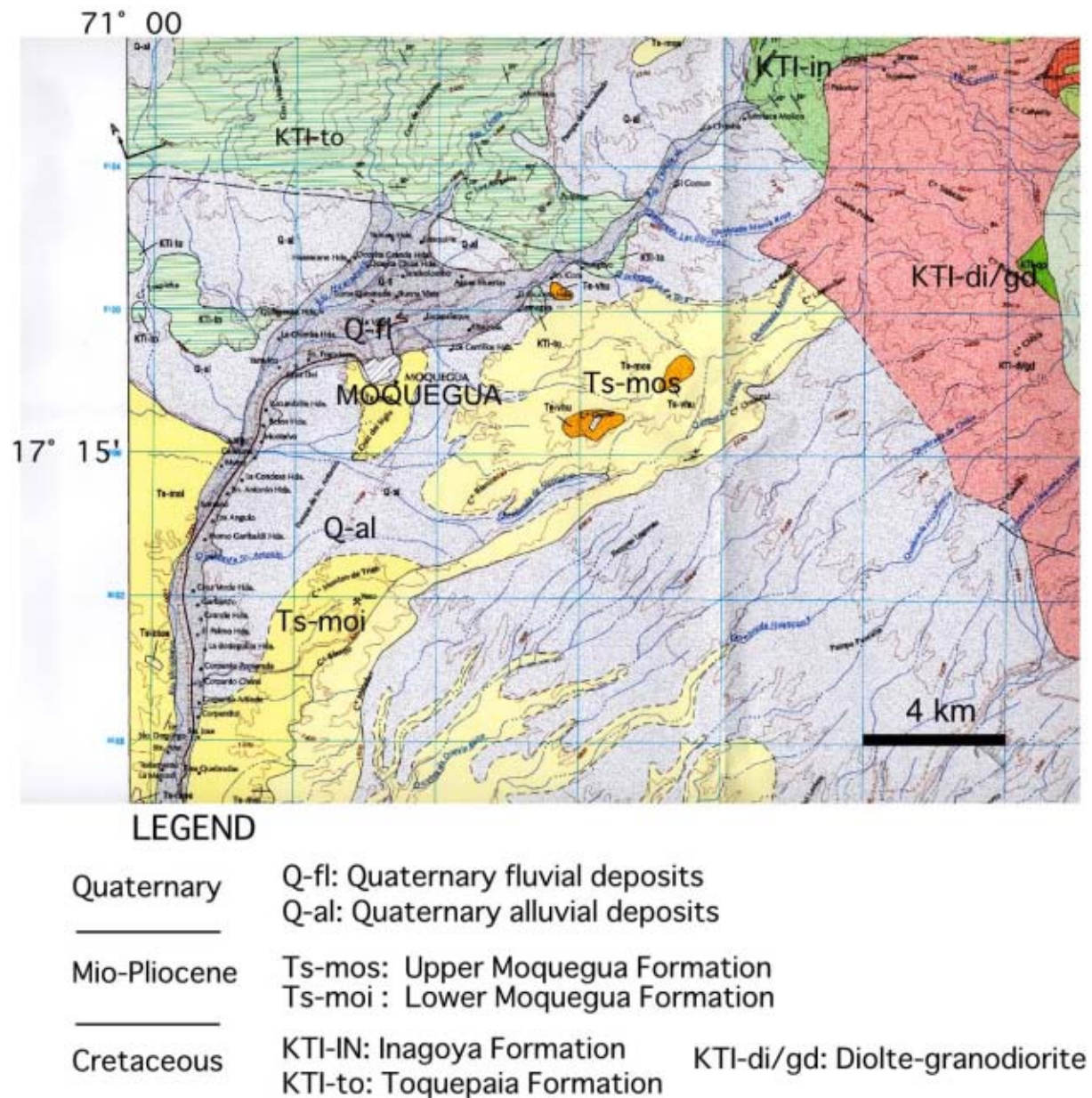
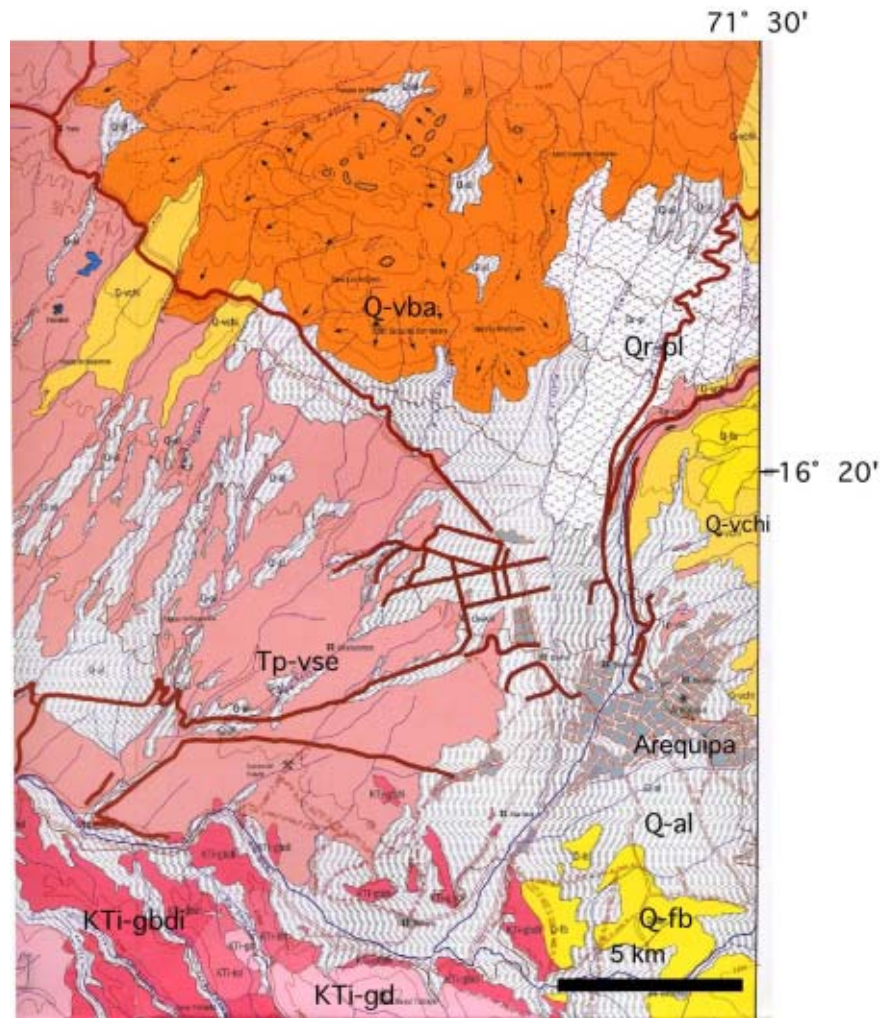


**Figure 2.16** Geological Map of Moquegua after Bellido and Landa (1998).

**AREQUIPA (Figure 2.17: Vargus, 1970)**

In the south of the city of Arequipa, Cretaceous igneous rocks are widely cropping out forming a seismic basement rocks. Around the city of Arequipa and its northern area, mainly Quaternary volcanic and volcanoclastic sediments are widely distributed. In the northern part of the city of Arequipa, Pliocene felsic tuff (Senca volcanics) is cropping out. Due to the covering of the Pliocene to Quaternary deposits, the actual depth of the Cretaceous rock in the city of Arequipa is not well understood.



Quaternary	Holocene	Q-al: alluvial deposits
	Pleistocene	Q-r-pl: pyroclastic flow deposits
	Pliocene	Q-fb: volcanoclastic deposits
	Cretaceous	Q-vba, Q-vchi: Barroso Group (andesitic volcanic products)
		Tp-vse: Senca volcanic products (felsic tuff)
		KTI-gbdi/KTI-gd: Cretaceous intrusive rocks (granodiorite, gabbro and diorite)

**Figure 2.17** Geological map of Arequipa after Vergus (1970).

## 2.5 SUMMARY

The Atico earthquake of June 23, 2001 (Mw 8.2-8.4) was an inter-plate subduction event between the Nazca and South American plates.

The sequential occurrence of great earthquakes since 1994 in southern Peru and northern Chile, suggests that the area between the rupture zones of the Atico earthquake 2001 and Antofagasta earthquake 1995 has a high seismic risk.

Only one strong ground motion record has been recovered from an instrument in the city of Moquegua. The influence of local geologic and soil conditions on the intensity of ground shaking, however, was clearly recognized through this reconnaissance. Topographical effects were thus evaluated in different ways in some seriously affected areas, microtremor measurements and plotting cracked utility poles on a map. Distribution of cracked utility poles is considered to be a good index for discussing possible spatial distribution of intense ground motions because they are all simple upright beams with the same materials, dimensions and structural details. Observed crack intensities on total 59 utility poles in San Francisco area, Moquegua, suggested that the mountain ridge might have amplified the ground motion, and thus was responsible for the damage to dwellings along the ridge. Observed H/V spectra of microtremors showed that there was a clear peak identified at around 4-5Hz, the fact indicating the topographical effect.

## ACKNOWLEDGMENT

We deeply appreciate to Prof. Jorge E. Alva Hurtado for suggesting the references of seismic activity in Peru.

(2.1, 2.2, 2.4, 2.5/ Hiroshi SATO, ERI, University of Tokyo)  
(2.3, 2.5/ Kazuo KONAGAI, Kimiro MEGURO & Paola MAYORCA IIS, University of Tokyo)

## REFERENCES

- Barazangi, M. and Isacks, B. (1979). "Subduction of the Nazca plate beneath Peru: evidence from spatial distribution of earthquakes." *Geophy. J. R. Astr. Soc.*, **57**, 537-555.
- Bellido, E. and Landa, E. (1998). "Mapa geologico cuadrangulo Moquegua." *Ministerio de Fomento Y O.P.*
- Bernal, I. (2000). "Carateristicas de la sismidad en la region sur de Peru." *Revista de Trabajos de Investigacion, CNDG-Biblioteca*, Institute Geofisco del Peru, p. 69-80.
- Comte, D. and Pardo, M. (1991). "Reappraisal of great historical earthquakes in the northern Chile and southern Peru seismic gaps." *Natural Hazards*, **4**, 23-44.
- Delous, B., Monfrest, T., Dorbath, L., Pardo, M., Rivera, L., Comte, D., Haessler, H., Caminade, J., Ponce, L., Kausel, E., and Cisternas, A. (1997). "Mw=8.0 Antofagasta (Northern Chile) earthquake of 30 July 1995: a precursor to the end of the large 1877 Gap." *Bull. Seismol. Soc. Am.*, **87**, 427-445.
- Dorbath, L., Cisternas, A. and Dorbath, C. (1990). "Assessment of the size of large historical earthquakes in Peru." *Bull. Seismol. Soc. Am.*, **88**, 551-576.
- Hasegawa, A. and Sacks, I. (1981). "Subduction of the Nazca Plate beneath Peru as detrmind from seismic observations." *Jour. Geophys. Res.*, **86**, 4971-4980.
- Jaen, H. and Oritiz, G. (1998). "Mapa geologico cuadrangulo Tacna." *Ministerio de Fomento Y O.P.*
- Kikuchi, M. and Yamanaka, Y. (2001). "The 23 June earthquake in Peru –An analysis of far field body waves (temporary solution)." in *EIC Seismological note Number 105*([http://www.eic.eri.u-tokyo.ac.jp/EIC/EIC\\_News/105E.html](http://www.eic.eri.u-tokyo.ac.jp/EIC/EIC_News/105E.html)).
- Kirby, S.H., Okal, E.A. and Engdahl, E.R. (1995). "The 9 June 94 Bolivian deep earthquake: an exceptional event in an extraordinary subduction zone." *Geophys. Res. Lett.* **22**, 2233-2236.
- Nakamura, T. (2000). "Clear Identification of fundamental idea of Nakamura's Technique and its

- applications.” *Proc., 12<sup>th</sup> World Conference on Earthquake Engineering*, 2656.
- Spence, W., Mendoza, C., Engdahl, E. R., Choy, G. L., and Norabuena, E. (1999). “Seismic subduction of the Nazca Ridge as shown by the 1996-1997 Peru earthquakes.” *Pure appl. Geophys.*, **154**, 753-776.
- Tavera, H. and Buforn, E. (1998). “Sismicidad y sismotectonica de Peru.” *Fisica de la Terra*, **10**, 187-219.
- Tavera, H., Salas, H., Jimenez, C. , Antayhua, Y., Vilcapoma, L., Millones, J., Bernal, I., Zamudio, Y., Carpio, J., Agüero, C., Perez-Pacheco, I. and Rodríguez, S. (2001). “El terremoto de Arequipa del Junio de 2001.” Instituto Geofísico del Peru, 16 p.
- Valgas, L. (1970). “Geología del cuadrangulo de Arequipa.” *Servicio de Geología y Minería Boletín*, **24**, 64p. with Geological Map sheet (1:100,000).



[to the next page](#)

